J Mol Model (2002) 8:184–190
DOI 10.1007/s00894-002-0085-x

ORIGINAL PAPER

Bohdan Koudelka · Pavla Capkova

Supramol – a program for structure analysis of intercalates using molecular simulations: the structure of $VOPO_4 \cdot C_6H_4O_2$

Received: 16 January 2002 / Accepted: 2 April 2002 / Published online: 29 May 2002

Abstract A method of structure analysis of intercalates has been developed that uses a combination of molecular simulations with powder diffraction. The program Supramol for the determination of intercalated structures uses crystal energy minimization in conjunction with powder diffraction data.

The program solves the multiple minima problem in molecular mechanics, generating initial models systematically and searching for the global energy minimum by comparing the experimental and calculated diffraction patterns. The program is compatible with the Cerius^2 modeling environment.

Two intercalated crystal structures solved by Supramol are presented in the present paper: vanadyl phosphate intercalated with *p*-benzoquinone and the high temperature phase of vanadyl phosphate intercalated with dioxane. The structure of vanadyl phosphate intercalated with *p*-benzochinone is tetragonal, space group *I*4/*m*, the unit cell parameters *a*=6.21 Å, *b*=6.21 Å, *c*=20.18 Å and the density is ρ=2.30 g cm^{-3}, *Z*=4. The crystal structure of vanadyl phosphate intercalated with dioxane (high temperature phase) is monoclinic, space group *C*2/*m*, unit cell parameters are: *a*=*b*=8.94 Å, *c*=8.22 Å, α=γ=90°, β=106.30°, *Z*=4, density 2.248 g cm^{-3}.

Keywords Intercalation · X-ray powder diffraction · Vanadyl phosphate · *p*-benzoquinone

Introduction

Molecular simulations represent a very powerful tool in the analysis of structures with a certain degree of disorder. In such a case it is usually not possible to produce single crystals of sufficient size and quality for conventional single crystal diffraction analysis. However, structure determination from powder diffraction data is complicated by a large overlap of reflections and, in addition, by the structural disorder and preferred orientation of crystallites. Then the combination of molecular simulations with powder diffraction provides a route to crystal structure determination. [1, 2, 3, 4] Especially the combination of energy calculation with *R*-factor calculation has been published in recent work. [5] In addition the new direct-space methods for the ab initio solution of crystal structures from powder diffraction data are presented in. [6, 7] An overview of these methods is presented in. [8]

In the present work we used this method to solve the crystal structures of intercalates. In the case of intercalates the host structure is built from rigid layers with covalent intralayer and weak interlayer bonding. Guest molecules intercalated into the interlayer space are non-covalently bonded to the host layers. The structure of the intercalate is a result of competition between the host–guest and guest–guest non-covalent interactions.

Intercalation is in fact the positioning of known molecules into a known crystal structure, i.e. the structure analysis of intercalates has to solve the following specific problems:

- To find the position, orientation, arrangement and possible conformational changes of guest molecules in the interlayer space.
- To describe the stacking of layers.
- As the intercalated layered structure usually exhibits a certain degree of disorder, the estimation of the character and degree of disorder is an integral part of the structure analysis.

The disorder that is usually present in intercalated layered structures leads to low resolution of X-ray diffraction diagrams. Due to the disorder the samples are usually available in powder form only. This means the quality of the X-ray diffraction pattern is additionaly affected by the preferred orientation and the absorption in surface

B. Koudelka (✉) · P. Capkova
Department of Chemical Physics and Optics,
Faculty of Mathematics and Physics,
Charles University Prague, Ke Karlovu 3,
121 16 Prague 2, Czech Republic
e-mail: koudelka@mbox.troja.mff.cuni.cz
Tel.: +42-21912510

roughness. In such a case molecular modeling represents a very useful tool in structure analysis.

The energy minimization routines employed by molecular mechanics simulations usually refine the starting geometry to a nearest local minimum, which is not necessarily the global minimum. The computational methods used to find the global minimum have to generate a large number of initial models with different starting geometries and can be divided into three groups: [9]

1. Deterministic or rigid search by systematically scanning the entire potential energy surface
2. Stochastic methods (Monte Carlo, Genetic Algorithms, [10, 11]...)
3. Molecular dynamics

The method presented in this paper is deterministic, using a combination of molecular mechanics with experimental powder diffraction data. The strategy is based on the specific features of the intercalated structures; i.e. the layers of the host structure and guest species are considered as rigid units in the first approximation. If IR spectroscopy does not confirm this assumption, then in the second stage the geometry of the guest molecules can be refined. The series of initial models is created by systematic rotations and translations of the guest molecules with respect to host layers and with respect to each other within one unit cell. Sub-rotations in the guest molecules can also be included to allow torsions in the bonding geometry. Selected properties (the integral intensity or positions of selected *hkl* peaks) of the X-ray powder pattern diffractogram are calculated for each initial model and compared with the experimental data. The total sublimation energy consisting of the van der Waals, electrostatic and hydrogen bond contribution is minimized only for the best fitting models. This method leads to a set of initial models which most accurately (as the first approximation) fit the experimental powder diffraction pattern. Finally, the disorder can be treated by an appropriate sum of the diffraction patterns correspondingly to the final minimized models, with nearly the same crystal energy.

How it works

At first we index the peaks in the diffraction pattern with appropriate *hkl* indices and determine the unit cell parameters and space group of the crystal. This can be done by standard indexing procedures. We also have to determine the number of molecules in the unit cell. This can be assessed from density considerations or solid-state NMR [12]. Once the unit cell parameters, symmetry group and cell contents are known, we define a *grid of initial models* that covers the entire space given by all degrees of freedom, i.e. positions, orientations and subrotations of the intercalated molecules. Each node of this grid represents a single initial model of the structure we search.

Selected quickly computable properties of the X-ray patterns, e.g. the relative integral intensity of some peaks, are computed for all the initial models and compared with experiment. The models with the best agreement (only a rough first approximation which is quickly computable – the well known Rietvelt X-ray refinement can usually be done after energy minimization at the end of the whole procedure) between experimental and calculated diffractograms are then passed to energy minimization within the one mesh of the grid.

The resulting structure with the lowest energy is then considered to be the global energy minimum. We can also compute the R_p factor to decide which model (from a group of models with quite low energy) best fits the diffraction data.

The grid of initial models

The rotations, sub-rotations and shifts of guest molecules in the unit cell are defined by the relative positions of selected atoms (e.g. rotation around a C–C bond) or by static vectors (e.g. rotation around *x* axes). Spherical coordinates (ϑ, ϕ) of rotations around a point with relative definition of poles are also implemented.

If the best descriptions of the desired movements and their ranges have been chosen for each intercalated molecule then we consider the size of the step of each movement with respect to the resulting number of initial models. Supramol can test about 100,000 models per second for selected properties of an X-ray diffractogram (Octane workstation with MIPS R10000 at 175 MHz). Thus, it is realistic to choose up to 10^8–10^{10} nodes of the grid. This allows two "usual" intercalated molecules in the unit cell to have a 5°–10° step in angle variables and 0.1 Å step in shifts.

Pre-computation of partial X-ray form factors *F* corresponding to every possible orientation of the rigid units within the model geometrically (with respect to a number of rigid units) speeds up the calculation and is also included in Supramol calculations.

Fulfilling the X-ray requirements

The intensities (relative integral intensities or heights of the peaks in diffraction pattern) I_k of the chosen reflection planes ($\mathbf{k}=2\pi[h\mathbf{a}^*+k\mathbf{b}^*+l\mathbf{c}^*]$ represents here a particular *hkl* reflection plain and $\mathbf{a}^*,\mathbf{b}^*,\mathbf{c}^*$ are the reciprocal lattice vectors.) can be calculated in all the nodes of the grid. The intensity of *hkl* reflection is given by

$$I_k = S_c C_{\mathbf{k}} |F_{\mathbf{k}}|^2 \quad \text{where} \quad F_{\mathbf{k}} = \sum_A f_A(|\mathbf{k}|) \exp(i\mathbf{k}\cdot\mathbf{r}_A) \qquad (1)$$

where S_c is the scale factor including all the factors that do not depend on the diffraction angle. The factor C_k denotes all the angle-dependent factors, which in the case of powder diffraction includes:

- the multiplicity factor and the Lorentz polarization factor
- surface absorption (due to the surface roughness [13])
- preferred orientation [14, 15, 16]

- the average isotropic Debye–Waller factor, which may include not only the effect of thermal vibrations but also the static displacement of atoms due to the disorder

Since the intensity is a smooth function of all the movement variables (atom coordinates $\mathbf{r}_A$ of each atom A in the unit cell), we can obtain an upper bound to the maximal change of intensity within one mesh (multidimensional polyhedron) of the grid ΔI_k, so we are able to determine whether the experimental value of I_k can be reached within one mesh or not. If this is so, the model is passed to energy minimization.

ΔI_k within one mesh of the grid

The maximum change of the intensity ΔI_k within one mesh of the grid is determined by the upper bound of its derivation. We now give some ideas on how to obtain such an upper bound, which can be pre-computed and used for the whole grid.

In order to simplify the explanation we use a simple two dimensional grid: one molecule in the model is rotated by an angle α and shifted by a distance β. The particular change of atom coordinates corresponding to the two movements can be described by derivations

$$\frac{\mathrm{d}\mathbf{r}_A}{\mathrm{d}\alpha} = \mathbf{o} \times \mathbf{r}_A \quad \text{and} \quad \frac{\mathrm{d}\mathbf{r}_A}{\mathrm{d}\beta}\mathbf{s}$$

where **o** is the axe of rotation and **s** the shift direction.

Using Eq. (1) we obtain

$$\frac{\mathrm{d}F_\mathbf{k}}{\mathrm{d}\alpha} = (\mathbf{k} \times \mathbf{o}) \cdot \nabla_\mathbf{k} F_\mathbf{k}^{\mathrm{mol}} \quad \text{and} \quad \frac{\mathrm{d}F_\mathbf{k}}{\mathrm{d}\beta} = i\mathbf{k} \cdot \mathbf{s} F_\mathbf{k}^{\mathrm{mol}} \tag{2}$$

where $F_\mathbf{k}^{\mathrm{mol}}$ denotes the part of $F_\mathbf{k}$ corresponding to the rotated (or shifted) molecule. The upper bound of $F_\mathbf{k}$ change within the mesh $\pm\Delta\alpha/2$, $\pm\Delta\beta/2$ is then

$$\Delta\Re F_\mathbf{k} = \max_{\mathbf{k},\mathbf{o}} \left| \Re \frac{\mathrm{d}F_\mathbf{k}}{\mathrm{d}\alpha} \right| \frac{\Delta\alpha}{2} + \max_{\mathbf{k},\mathbf{s}} \left| \Re \frac{\mathrm{d}F_\mathbf{k}}{\mathrm{d}\beta} \right| \frac{\Delta\beta}{2} \tag{3}$$

also for the imaginary part. The maximization is performed in such a range of relative positions of vectors **o**, **k** and **s** according to the atomic coordinates of the molecule in the basic state that it contains the whole grid of models. Consequently

$$\Delta I_k = S_c C_k \left\{ (|\Re F_\mathbf{k}| + |\Delta\Re F_\mathbf{k}|)^2 - (\Re F_\mathbf{k})^2 + (|\Re F_\mathbf{k}| + \Delta\Re F_\mathbf{k})^2 - (\Re F_\mathbf{k})^2 \right\}$$

A complete detailed description of all the mathematical routines will be published separately as it is beyond the range of this publication.

Energy minimization

As a first approximation we minimize the structure energy with respect to van der Waals (vdW) interactions (calculated using Lenard-Jones potentials) which defines a "good" packing of molecules within a unit cell. Only the models with vdW energy under e.g. 100 kcal mol^{-1} can be used as initial models for further Cerius^2 (or other more sophisticated) minimization. For such a rough vdW calculation we use a special fast algorithm.

This minimization is applied to each node of the grid of models that satisfies the X-ray requirements. It is done only within the range of the size of one step of each molecular movement – the multidimensional polyhedron in the state space of the crystal.

Using Supramol with Cerius^2

The Supramol program was developed as an extension of the software package Cerius^2, but can also work as a standalone application. The two software packages communicate via *.msi and *.trj files. The relative definitions (with respect to selected atom positions) of movements of intercalated molecules can be done by the MEASUREMENTS module in the graphical Cerius^2 environment.

The set of the best initial models generated by Supramol is passed to the final crystal energy minimization using the module Crystal Packer in Cerius^2. Energy calculations in Crystal Packer take into account the non-bond terms only, i.e. van der Waals interactions (VDW), Coulombic interactions (COUL) – charges are calculated using the Charge equilibrium method – [17] hydrogen bonding (H-B), internal rotations and hydrostatic pressure. The asymmetric unit of the crystal structure is divided into fragment-based rigid units. Non-bond (VDW, COUL, H-B) energies are calculated between the rigid units. During energy minimization, the rigid units can be translated and rotated and the unit cell parameters varied. In our case we used VDW interactions with the Tripos 5.2 force field. [18] As a result we obtain the structure models corresponding to the lowest energy. Then we use the R_p factor (in Cerius^2 module Analytical 1 – X-ray calculation – Powder)

$$R_\mathrm{p} = \frac{\sum_k \left(I_k^{\mathrm{exp}} - I_k^{\mathrm{calc}}\right)}{\sum_k I_k^{\mathrm{exp}}}$$

to decide which of the final models fits the experimental diffraction data.

$VOPO_4$ intercalated with *p*-benzoquinone; results and discussion

The program Supramol was used successfully to determine the crystal structure of vanadyl phosphate intercalated with *p*-benzoquinone.

Host structure of vanadyl phosphate

Figure 1 describes the host structure of vanadyl phosphate dihydrate $VOPO_4 \cdot 2H_2O$, which was determined by

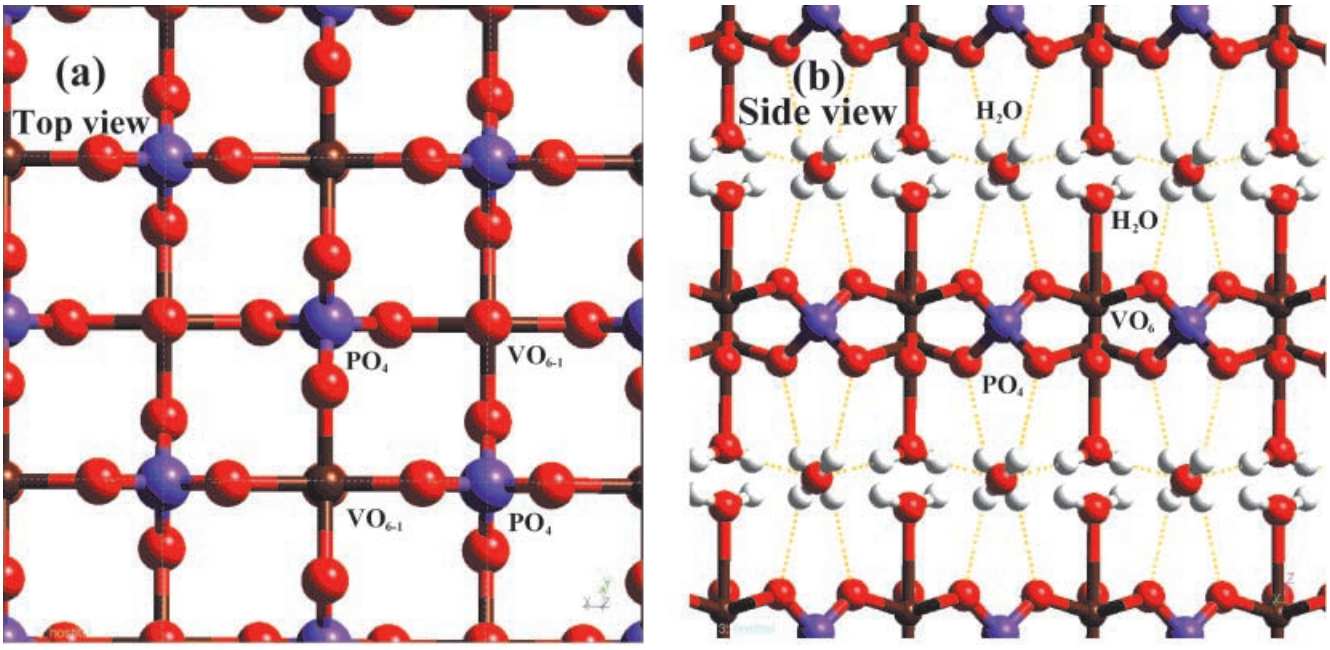

Fig. 1 The view of the host structure of vanadyl phosphate dihydrate $VOPO_4 \cdot 2H_2O$. **a** Top view. **b** Side view. Colour of atoms: V – *brown*, O – *red*, P – *purple*, H – *white*

Tietze et al. [19] from single-crystal diffraction data as tetragonal, space group *P*4/*nmm* with *a*=6.202 A, *c*=7.41 A and *Z*=2. Tachez et al. [20] presented the results of structure refinement of the deuterated compound $VOPO_4 \times \cdot 2D_2O$ based on neutron powder diffraction data: space group *P*4/*n*, *a*=6.2154 Å, *c*=7.4029 Å and *Z*=2. The host structure of vanadyl phosphate consists of infinite sheets of distorted VO_6 octahedra and PO_4 tetrahedra linked by shared oxygen atoms (see Fig. 1a). Shared water molecules link these sheets together, creating a regular network of hydrogen bridges in the interlayer space (Fig. 1b). As one can see from Fig. 1b, there are two differently bonded water molecules in the interlayer space: one water molecule is attached with its oxygen to vanadium to complete the VO_6 octahedron and the second one is hydrogen bonded to PO_4 oxygens and to the first water molecule. Both water molecules occur in two symmetry-equivalent orientations with occupancy 0.5, which means that two equivalent networks of hydrogen bonds occur in the interlayer space corresponding to two orientations of the water molecules. (For a more detailed description of the host structure see Tachez et al. [20]) This kind of interlayer arrangement of water molecules with two possible orientations can also occur in the arrangement of intercalated species. Interlayer water in the host structure $VOPO_4 \cdot 2H_2O$ is very weakly bonded and can be replaced easily by organic molecules. Then the intercalated molecules must deliver their oxygen atoms to complete the VO_6 octahedra. This means that the empty apex of the VO_6 octahedron represents a strong active site for anchoring the organic molecule via its oxygen atom.

Intercalation with *p*-benzochinone

The structure of vanadyl phosphate intercalated with *p*-benzoquinone is tetragonal, space group *I*4/*m*, the unit cell parameters *a*=6.21 Å, *b*=6.21 Å, *c*=20.18 Å and the density is ρ=2.30 g cm^{-3}, *Z*=4. The intercalation causes several changes in the crystal structure. Firstly, in the intercalate the two successive host layers are mutually shifted by a vector **a**/2+**b**/2 in comparison with the host structure. Consequently, the space group changes from *P*4/*n* to *I*4/*m*. Secondly, each pair of water molecules is replaced by one molecule of *p*-benzoquinone. The vanadium octahedron is completed by the oxygen atom of a *p*-benzoquinone molecule, which means that *p*-benzoquinone is anchored to vanadium via its oxygen atom. The V–O distance found by Supramol is 2.31 Å.

The layer fourfold axis going through the vanadium atom in the *z* direction determines the symmetry of the whole intercalate. Each *p*-benzoquinone molecule can reside in four equivalent positions with occupancy 1/4 (see Fig. 2). This disorder makes the experimental electron density map in the interlayer space rather fuzzy and unusable for determining the position of each individual atom in the unit cell. Molecular modeling is often a great help in these cases and Supramol makes it even more powerful and successful.

The side view of the final structure is shown in Fig. 3, where one can see a real arrangement of *p*-benzoquinone in the interlayer space. The fractional atomic coordinates and occupancy factors of the final crystal structure are listed in Table 1.

A comparison of experimental and calculated diffraction patterns is shown in Fig. 4. The experimental pattern was transformed as follows. (1) Background noise was removed by subtracting a five-order polynomial and by broadening with Gaussians of 0.3 width. (2) March–Dollase correction for the preferred orientation with the

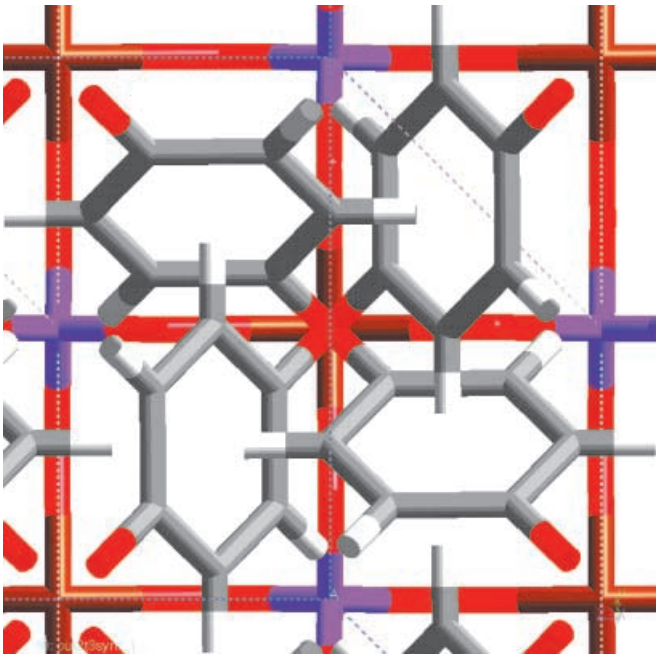

Fig. 2 $VOPO_4 \cdot C_6H_4O_2$ Anchoring of the *p*-benzoquinone molecule to the host layers (top view). The fourfold axis of symmetry in V–O bond atoms makes each of the *p*-benzoquinone positions symmetrically equivalent. In reality there is always one molecule only, but in calculating the X-ray diffractogram all of the positions with occupancy factor 1/4 must be taken into account. Colour of bond sticks: V – *brown*, O – *red*, P – *purple*, H – *white*, C – *black*

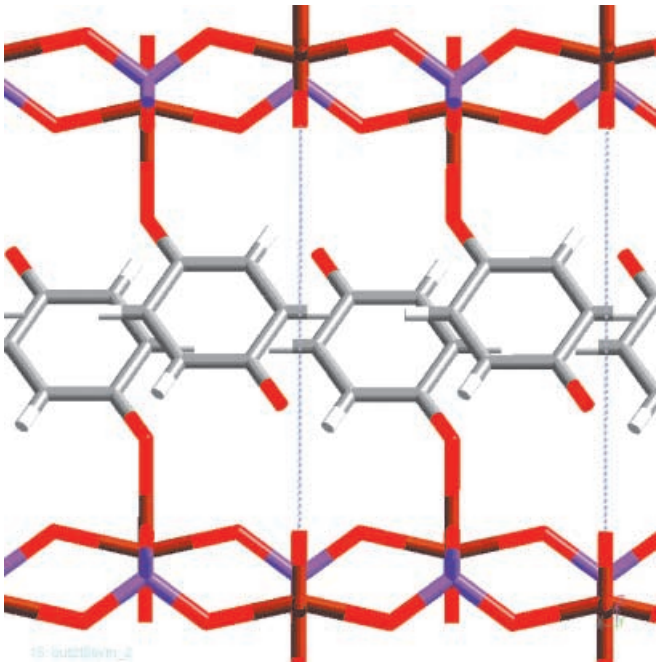

Fig. 3 Side view of $VOPO_4$ $C_6H_4O_2$, structure, showing the monolayer arrangement of *p*-benzoquinone molecules in the interlayer space of $VOPO_4$. The realistic model (only one of the four possible positions of *p*-benzoquinone presented) of mutual position of *p*-benzoquinone molecules corresponds to the energy minimum. Colour of bond sticks: V – *brown*, O – *red*, P – *purple*, H – *white*, C – *black*

Table 1 Atomic fractional coordinates and occupancy factors of $VOPO_4 \cdot C_6H_4O_2$

*I*4/*m* Atom	*a*=6.21 Å *u*	*b*=6.21 Å *v*	*c*=20.18 Å *w*	*N*
layer				
V	0.000	0.000	–0.225	1
O	0.000	0.000	–0.296	1
P	0.500	0.000	–0.250	1
O	0.499	–0.200	–0.295	1
p-benzoquinone				
O	0.000	0.000	–0.111	0.25
O	0.442	–0.429	0.078	0.25
C	0.447	–0.213	–0.017	0.25
C	0.332	–0.101	–0.066	0.25
C	–0.004	–0.216	–0.016	0.25
C	0.107	–0.103	–0.065	0.25
C	0.110	–0.328	0.033	0.25
C	0.336	–0.326	0.033	0.25
H	–0.157	–0.218	–0.016	0.25
H	0.600	–0.212	–0.017	0.25
H	0.408	–0.025	–0.099	0.25
H	0.035	–0.404	0.067	0.25

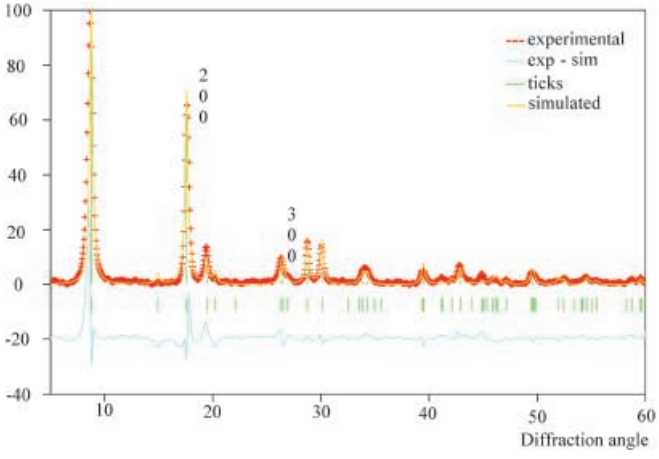

Fig. 4 Comparison of computed diffraction pattern of $VOPO_4$ $C_6H_4O_2$ (*yellow solid line*) and experimental one (*red crosses*) – dependency of X-ray scattering intensity *I* on the 2ϑ scattering angle. Subtraction of both is visualized by the blue solid line at the bottom. X-ray wavelength λ=1.5418 Å

texture axis in the *z* (perpendicular to layers) direction with R_0=0.8 was used. The resulting R_p factor is R_p=9.1%.

The powder data of the intercalate were measured using an X-ray powder diffractometer (HZG-4, Germany) using Cu $K_{\alpha 1,\,\alpha 2}$ radiation (λ=1.5418 Å) with discrimination of the Cu K_β by an Ni filter. Silicon (*a*=5.43055 Å) was used as external standard. The diffraction pattern was measured in the angle range $2\vartheta \subset \langle 5°, 60° \rangle$ No measurable reflections were detected for 2ϑ=60°. One reason for this effect is the strong preferred orientation in the powder sample suppressing the *hkl* reflections. The second reason for the low quality of the diffraction pattern is the positional disorder of the guest molecules, which

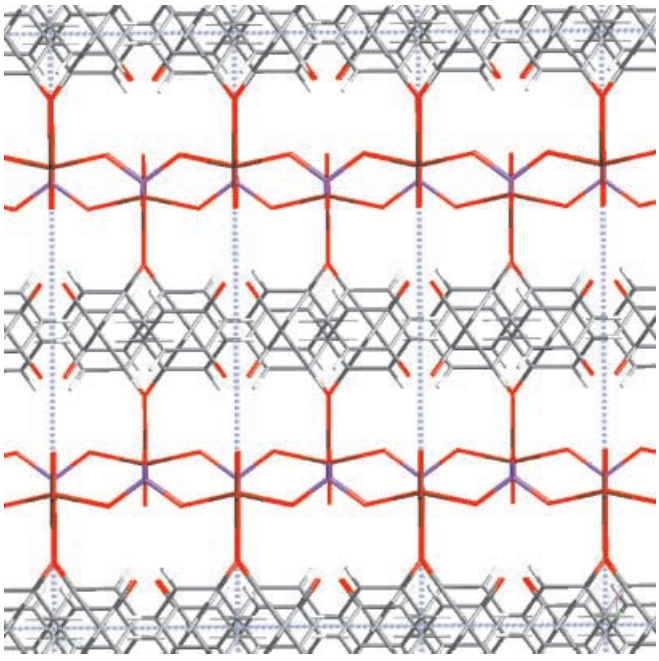

Fig. 5 Side view of $VOPO_4$ $C_6H_4O_2$ structure, showing all possible equivalent positions of *p*-benzoquinone molecules in *I*4/*m* symmetry. Colour of bond sticks: V – *brown*, O – *red*, P – *purple*, H – *white*, C – *black*

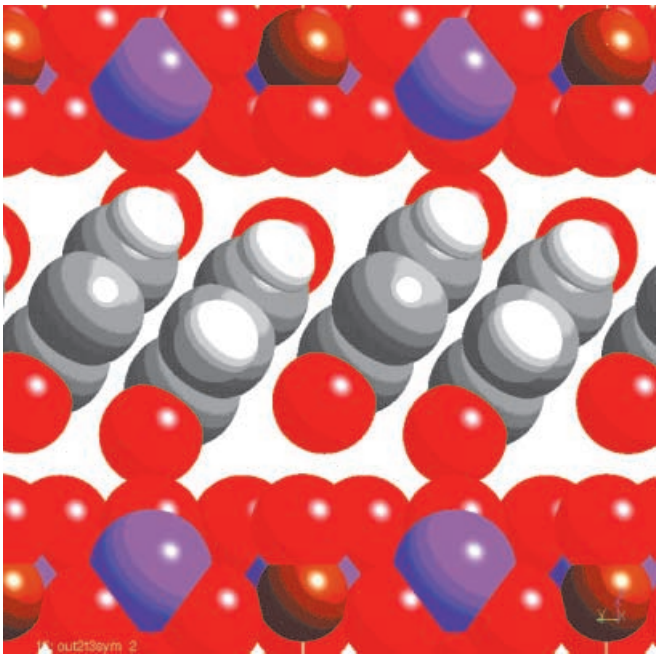

Fig. 6 Side view of $VOPO_4$ $C_6H_4O_2$ structure visualized using Van der Waals radii in order to illustrate the inter-layer space filling. Colour of atoms: V – *brown*, O – *red*, P – *purple*, H – *white*, C – *black*

leads in the real structure to the existence of domains where only one quarter of the *p*-benzoquinone positions are occupied. The strain at domain boundaries causes the diffraction profile broadening and in general results in low resolution of the diffraction pattern.

Finally, Fig. 5 introduces the *I*4/*m* symmetry of the crystal and Fig. 6 shows the atomic VdW radii and filling of the space.

Intercalation with dioxane

The high temperature phase of vanadyl phosphate intercalated with dioxane $VOPO_4 \cdot (1/2)C_4H_8O_2$ existing above 50 °C is monoclinic, space group *C*2/*m*, unit cell parameters are: $a=b=8.94$ Å, $c=8.22$ Å, $\alpha=\gamma=90°$, $\beta=106.30°$, $Z=4$ (four formula units per one unit cell), and the density is 2.248 g cm^{-3}. Molecules of dioxane in chair-like conformations are anchored to vanadium in the lower and upper layers of $VOPO_4$ via oxygen (see Fig. 7). The V–O distance found by Supramol is 2.495 Å, and the basal spacing is 7.89 Å. Figure 7 shows the side view of the monolayer arrangement of dioxane molecules. The top view, showing the ordering of guests in the inter-layer space, is shown in Fig. 8. Comparing Figs. 2 and 8, one can see the mutual shift of two successive VOPO4 layers along the diagonal direction **a**+**b**. The fractional coordinates in the unit cell for the high temperature phase of $VOPO_4 \cdot (1/2)C_4H_8O_2$ are summarized in Table 2. The R_p factor in this case is 6.7% after the correction of diffraction data for the preferred orientation according to March and Dollase [16].

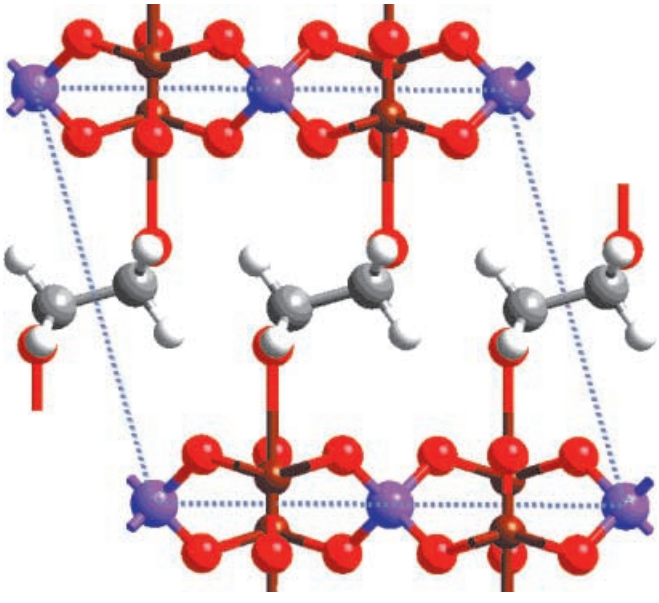

Fig. 7 High temperature phase of vanadyl phosphate intercalated with dioxane in side view showing the anchoring of the guest molecules to the lower and upper host layer. Colour of atoms: V – *brown*, O – *red*, P – *purple*, H – *white*, C – *black*

Conclusions

The present results show that the program Supramol makes structure determination faster, more effective and more reliable than the standard procedure using manual-

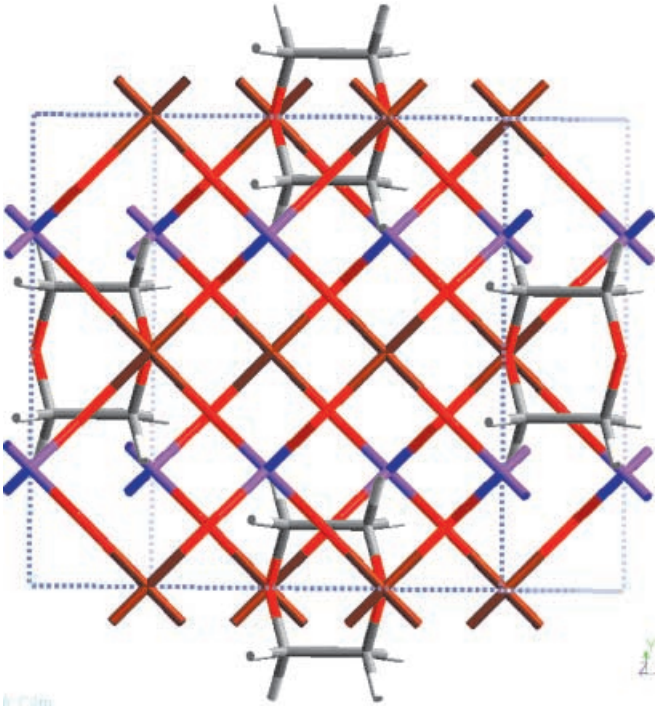

Fig. 8 Top view of the structure of vanadyl phosphate intercalated with dioxane shows the arrangement of guest molecules in the interlayer space and mutual position of two successive host layers. Colour of atoms: V – *brown*, O – *red*, P – *purple*, H – *white*, C – *black*

Table 2 The fractional coordinates in unit cell for the high temperature phase $VOPO_4 \cdot (1/2)C_4H_8O_2$

*C*2/*m*	*a*=8.94 Å	*b*=8.94 Å	*c*=8.22 Å
Atom	*u*	*v*	*w*
P1	0.50000	–0.25043	0.00000
O1	0.28081	–0.50000	0.11931
V1	0.23324	–0.50000	–0.06491
O2	0.63106	–0.34893	0.11835
O3	0.43006	–0.15193	0.11835
C1	–0.09268	–0.63440	–0.52755
O4	0.15160	–0.50000	–0.38113
H1	–0.13668	–0.64433	–0.41235
H2	–0.14079	–0.73288	–0.61105

ly created initial models for energy minimization and comparing the diffraction data only as a final step of testing the result.

Concerning the intercalation of *p*-benzoquinone to vanadyl phosphate, we tried to set the initial model of the unit cell manually and minimize its energy by Cerius[2]. It seemed impossible to fulfil the given X-ray pattern. Finally, the program Supramol was successful at this task and we could determine the structure, which fits the experimental X-ray pattern by R_p=9.1%.

References

1. Erk P (1999) Crystal design, from molecular to application properties. In: Braga D, Orpen G (eds) Crystal engineering: from molecules and crystals to materials. Kluwer, Dordrecht, pp 143–161
2. Karfunkel HR, Rohde B, Leusen FJJ, Gdanitz RJ, Rihs G (1993) J Comput Chem 14:1125–1135
3. Engel GE, Wilke S, König O, Harris KD, Leusen FJJ (1999) J Appl Crystallogr 32:1169–1179
4. Hammond RB, Roberts KJ, Docherty R, Edmondson M (1997) J Phys Chem B 101:6532–6536
5. Lanning OJ, Habershon S, Harris KDM, Johnston RL, Kariuki BM, Tedesco E, Turner GW (2000) Chem Phys Lett 317:296–303
6. Woodley SM, Battle PD, Gale JD, Catlow CRA (1999) PCCP 1:2535–2542
7. Putz H, Schon JC, Jansen M (1999) J Appl Crystallogr 32: 864–870
8. Schon JC, Jansen M (2001) Z Kristallogr 216:361–383
9. Comba P, Hambley TW (1995) Molecular modelling of inorganic compounds. VCH, Weinheim, pp 1–58
10. Harris KDM, Kariuki BM, Johnston RL (1998) Adv Struct Anal 190–204
11. Shankland K, David WIF, Csoka T (1997) Z Kristallogr 212: 550–552
12. Thomas JM, Klinovski J, Rambadas S, Hunter BK (1983) Chem Phys Lett 102:158–162
13. Janeba D, Capkova P, Weiss Z, Schenk H (1998) Clays Clay Miner 46:63–68
14. Capkova P, Peschar R, Schenk H (1993) J Appl Crystallogr 26:449–452
15. Capkova P, Valvoda V (1974) Czech J Phys 24:891–900
16. Dollase WA (1986) J Appl Crystallogr 19:267–272
17. Rappe AK, Goddard WA III (1991) J Phys Chem 95:3358–3363
18. Clark M, Cramer III RD, Van Opdenbosh N (1989) J Comput Chem 10:982–1012
19. Tietze HR (1981) Aust J Chem 34:2035–2038
20. Tachez M, Theobald F, Bernard J, Hewat AW (1982) Revue Chim Miner 19:291–300